Supporting Information

Organic Solvent-Free, One-Step Engineering of Graphene-Based Magnetic-Responsive Hybrids Using Design of Experiment-Driven Mechanochemistry

Kuo-Ching Mei,† Yukuang Guo,† Jie Bai,† Pedro M. Costa,† Houmam Kafa,† Andrea Protti,‡ Robert C. Hider,† and Khuloud T. Al-Jamal†

† Institute of Pharmaceutical Science, King's College London, Franklin-Wilkins Building, 150 Stamford Street, London SE1 9NH, United Kingdom

‡ Cardiovascular Division, James Black Centre, King's College London British Heart Foundation Centre of Excellence, London SE5 9NU, United Kingdom

Keywords: graphene, mechanochemistry, DoE, SPIO, formulation, nanomedicine, drug delivery, toxicity

Materials

Graphite powder (cat: SP-1, batch: 04100, lot: 011705) was purchased from Bay Carbon, Inc. (USA). H_2O_2 (cat: 202460010) and HNO_3 (cat: 1244660011) were purchased from Acros Organics (USA). Isopore™ membrane, polycarbonate, hydrophilic, 0.22 μm (cat: GTTP04700) were ordered from Merck Millipore (UK). Agarose (cat: A5093), HCl (cat: 258148), $NaNO_3$ (cat: 221341), $KMnO_4$ (cat: 60459), $MgSO_4$ anhydrous (cat: 208094), and P_2O_5 (cat: 214701) were all obtained from Sigma-Aldrich (UK). Oleic acid coated hydrophobic SPIOs (with a size of 10 nm at 10^{17} particles per ml) were purchased from Magnacol Ltd., (UK), PTFE grinding jar (25 mL) was purchased from Retsch (Germany). Magnet (F329, 42 × 8 × 10 mm thick N42 Neodymium Magnet - 10.4 kg Pull) was obtained from Magnet Expert Ltd., (UK). GO was prepared using modified Kovtyukhova-Hammer's method.[1] Fetal bovine serum (FBS) was obtained from First-Link, UK Ltd, Advanced RPMI 1640 (containing 2000 mg/L glucose, 110 mg/L sodium pyruvate and non-essential aminoacids), Penicillin-Streptomycin 100X, 0.05% Trypsin-EDTA (1X) with Phenol Red, GlutaMAX™ Supplement were obtained from Invitrogen, Life Sciences, UK. CytoTox 96® Non-Radioactive Cytotoxicity Assay was obtained from Promega Corporation, UK.

Experimental Section

Synthesis of graphene oxide

Graphene oxide (GO) was prepared using the following procedures: graphite powder (4 g), potassium persulfate ($K_2S_2O_8$, 2 g) powder, and phosphorus pentoxide (P_2O_2, 2 g) were dry-mixed in a 250 mL round bottom flask followed by the addition of sulfuric acid (H_2SO_4, 96 ~ 98%, 6 ~ 10 mL). The mixture was stirred and refluxed for 6 hours at 80°C, cooled down to room temperature then diluted carefully in deionized water (DI H_2O). The mixture was then washed by filtration using a Millipore® All-Glass 47 mm Vacuum Filter Unit and hydrophilic polycarbonate Isopore™ membrane (0.22 μm) until the filtrate became pH neutral. The filter cake was oven dried at 40°C overnight to afford a black-gray powder. Dried pre-oxidised graphite powder (~ 4 g) and sodium nitrate powder ($NaNO_3$, 4 g) was dry-mixed in a 500 mL round bottom flask. Sulfuric acid (H_2SO_4, 96 ~ 98%, ~ 100 mL) was added and the mixture was kept stirring at 0°C on an ice bath. The mixture was agitated from time to time to avoid aggregation. The

temperature was monitored using a thermometer throughout the reaction. When the powders were fully dispersed, potassium permanganate powder ($KMnO_4$, 12 g) was added slowly (portion-wise) to the suspension. The addition rate was carefully controlled so that the temperature of the suspension was kept below 20°C. After the addition of $KMnO_4$ was complete, the suspension was stirred on an ice bath (0 ~ 10°C) for an additional 10 minutes. The ice bath was then removed and replaced with a water bath to allow the temperature to raise gradually to 35 ± 3°C. The temperature was maintained for at least 2 hr until the dispersion became a brown pasty mixture. The mixture was then heated to 60°C. When the temperature reached 60°C, 50 mL of DI H_2O was added to the pasty mixture and stirred for 5 minutes. The temperature was then set to 80°C followed by the addition of 50 mL of DI H_2O. When the temperature reached 80°C, 80 mL of DI H_2O was added to the mixture. A white vapour was generated. When the water addition was complete, the temperature was maintained above 80°C (temperature fluctuated between 80-95°C) and kept stirring for another 30 minutes. To stop the reaction, hydrogen peroxide (H_2O_2) aqueous solution (35%, 10 mL) was added to the mixture, which was then kept stirring for 30 minutes at 80°C. H_2O_2 reduces the residual manganese dioxide (MnO_2) and permanganate (MnO_4^-) forming a brown suspension. The warm brown suspension from the previous step was transferred into 10 × 50 mL conical-bottom centrifuge tubes and centrifuged at 3,214 × g (3900 rpm) for 2 minutes. The supernatant was removed and the pellets were re-suspended in 1N HCl using a spatula with agitation. The centrifugation and washing steps were repeated several times with 1N HCl (1L) followed by 1N NaOH (0.5 ~ 1 L). The washing and centrifugation steps were monitored by observing the colour of the supernatant. The colour changed from yellow-green (early HCl washing stage), nearly transparent (late HCl washing stage), light brown (early NaOH washing stage) and finally to dark brown when NaOH washing was stopped. The pellets were re-suspended in DI H_2O. Washing and centrifugation steps were repeated twice. The pellets were finally re-suspended in DI H_2O (50 mL/tube) and bath sonicated for 1 hr (USC300TH, VWR, Belgium). The sonicated mixture was centrifuged once at 3,214 × g (3900 rpm) for 2 minutes. GO suspension was obtained by strongly hand- shaking the centrifuge tubes and the supernatant was collected. Oxidized-graphite remained as pellet no matter how hard the shaking was. The collected supernatant was then diluted with DI H_2O (volume was not critical) forming a dark-brown GO suspension. The final concentration of GO in the

dispersion was determined by TGA as described in the main text using **Equation 6.** The dispersion concentration for as-synthesised GO stock was 6 mg/mL

Hybrid preparation by ball milling

GO and SPIOs were loaded into the grinding jar with four 12 mm stainless steel grinding balls (Retsch®, Germany). The milling process was performed *via* a high-speed vibrational ball-mill (MM 200 mixer mill, Retsch®, Germany). The initial GO/SPIOs wt/wt% ($RP_{Initial}$) was calculated as expressed in **Equation 5**, where $MS_{Initial}$ is the initial SPIOs weight (mg) loaded into the milling jar. The batch size of GO was fixed at 30 mg.

$$RP_{Initial} = \frac{30\ mg}{MS_{Initial}} \times 100\% \quad \textbf{(5)}$$

After milling, the mixture was recovered from the grinding jar by rinsing with 30 ml DI H_2O, then transferred into a 50 mL self-standing conical bottomed centrifuge tube. The majority of insoluble SPIOs remained in the jar (firmly attached to the wall of the jar). The dispersion was allowed to stand for 2 minutes to precipitate remaining free SPIOs. A magnet was then put in contact with the exterior of the tube at its middle part and left for 30 second. The magnetic hybrid was attracted to the magnet while non-magnetic GO remained in suspension. The non-magnetic fraction or any precipitates were discarded. The magnetic fraction was collected and re-suspended in 30 mL DI H_2O, and magnetic separation step was repeated once. After the final washing, the purified GO/SPIO hybrids was re-suspended in DI H_2O and stored at room temperature.

Thermogravimetric analysis (TGA)

TGA (TGA Q5000, TA Instruments, USA) was used to analyse both the final weight of the collected hybrid and the SPIOs content in each sample. Samples were run isothermally at 120 °C under nitrogen atmosphere for 2 min to allow for water removal so that the weight of the dried hybrid can be calculated. The concentration of hybrid in the original dispersion was calculated accordingly using **Equation 6**, where C is the concentration (mg/mL), V_L is the volume (µL) of dispersion being loaded on the TGA pan. The dried hybrid weight, generated from ball milling, was calculated using **Equation 7**, where M_{Total} is the total hybrid weight (mg) and V_{Total} is the total sample volume (mL).

$$C = M_1 \times \frac{V_L}{1000} \quad \textbf{(6)}$$

$$M_{Total} = C \times V_{Total} \quad \textbf{(7)}$$

The dried GO, SPIOs or GO/SPIO hybrids were then equilibrated at 100°C for 20 minutes before heating up with a ramp of 10°C /min from 100 to 900°C under compressed air with a flow rate of 90 mL/min. The residual weight (mg) after decomposition in compressed air was assigned as M_2. The weight (mg) of SPIOs (MS_{Final}) and GO (MG_{Final}) in the hybrid was calculated using **Equation 8a** and **8b**, respectively. As mentioned earlier, oleic acid coated SPIOs showed a weight loss of 31.48 ± 0.01 % at 800°C (n = 3). The value of M_2 was divided by 0.685 to account for oleic acid content in the coated SPIOs.

$$MS_{Final} = M_2/0.685 \quad \textbf{(8a)}$$

$$MG_{Final} = M_1 - MS_{Final} \quad \textbf{(8b)}$$

MS_{Final} and MG_{Final} values were used to calculate the final GO/SPIO wt/wt% (RP_{Final}) using **Equation 8c**.

$$RP_{Final} = \frac{MG_{Final}}{MS_{Final}} \times 100\% \quad \textbf{(8c)}$$

Atomic force microscopy (AFM)

The surface topography of GO samples deposited on a dry mica surface was studied with AFM using tapping mode. GO samples were prepared at a concentration of 0.2 mg/mL in water, deposited on the mica for 3-5 minutes. Excess sample was removed and the mica was dried under a gentle flow of compressed nitrogen (or a dust-free compressed air spray). The sampling was achieved by oscillating the tapping probe to hit the sample surface, which allowed short-time interactions with minimal shear force applied on the surface. The oscillation of reflected laser spot signal from the probe cantilever (general purpose tips cat: NSC15/AL, Mikromasch, USA) was collected with ScanAsyst® Dimension Icon® AFM (Bruker, UK). The AFM images visualization and analysis were achieved using Gwyddion v.2.39 (Department of Nanotechnology, Czech Metrology Institute, CZ).[2]

GO flake surface area analysis

The surface area of the GO flake was analysed using Image J 1.49i software from National Institute of Health (USA). Images from AFM were used for analysis with a total measurement number no less than 100 flakes. Histogram of surface area distribution and statistical calculation was generated and performed using DataGraph 3.1 (Visual Data Tools, Inc., USA).

Transmission electron microscopy (TEM)

TEM was performed on Philips CM 12 (FEI Electron Optics, The Netherlands) equipped with Tungsten filament and a Veleta - 2k × 2k side-mounted TEM CCD Camera (Olympus, Japan). The accelerating voltage was 80 KV. The spot size was set at 3. Objective aperture was used with all samples. GO-SPIOs aqueous dispersions at a concentration of 0.2 mg/mL were deposited on carbon-film on 300 mesh copper grids or lacey carbon films on 300 mesh copper grids for the measurement.

Attenuated Total Reflectance Fourier Transform Infrared (ATR- FTIR)

ATR-FTIR was performed using PerkinElmer® Frontier™ FT-IR equipped with ATR accessory (diamond ATR polarization accessory with 1 reflection top-plate and pressure arm). The pressure arm was used for all solid samples at a force gauge setting between 100-120 units; no compression was used for liquid/oil samples. The number of scans was set at 15. Samples were loaded on the reflection top-plate at a quantity sufficient enough to cover the entire diamond surface. GO/SPIO hybrids were dispersed in water and freeze dried into a loose sponge-like structure. The container was sealed immediately after freeze-drying. Samples were warmed to room temperature before the measurement to minimise moisture absorption, in order to obtain a good spectrum resolution with minimum interferences.

Raman spectroscopy

Raman spectroscopy was performed using Renishaw® inVia-Reflex spectrometer (UK) with an excitation wavelength set to 785 nm and 0.1 to 50 % laser power. SPIOs and

GO/SPIO hybrids were deposited on a calcium fluoride (CaF_2) slide (Crystran Ltd, UK). Acetone was used to disperse the sample on the slide and was removed by air-dry at room temperature. Measurements were performed from 500 cm^{-1} to 3200 cm^{-1} for each sample (n = 3). To boost the Raman signal of the SPIOs, higher laser power was used to transform the SPIOs into α-Fe_2O_3. In brief, GO/SPIO hybrids were firstly bleached with 50 % laser power for 30 seconds followed by 1 % laser power for 30 seconds. Raman spectra were then obtained using 1 % laser power with 5 accumulative scans for one sample. The final spectrum of GO/SPIOs was obtained by averaging the signal from 3 measurements then normalisation to the GO's G band intensity. Data were acquired and analysed using Renishaw's WiRE 4.0 (Windows-based Raman Environment) software.

The modified Lactate dehydrogenase (LDH) assay for *in vitro* toxicity assessment

J774 (murine macrocytes) and A549 cells (adenocarcinomic human alveolar basal epithelial cells) were used for *in vitro* toxicity assessment of the GO/SPIO hybrids. Cells were maintained in Advanced RPMI 1640 medium, supplemented with 10% heat-inactivated FBS, 100 U/mL penicillin, 100 μg/mL streptomycin, 2 mM GlutaMax and cultured at 37 °C under a humidified atmosphere containing 5 % CO_2. J774 and A549 cells were seeded onto 96-well plates (1.5 x 10^4 cells per well) and allowed to divide for 24 hr. The dispersions of GO/SPIO hybrids, prepared in distilled water, were then added onto the cells at a final "SPIOs" concentration of 10, 25, 50 or 100 μg/ml. After 24 and 72 hr, light microscopy images were captured (10X optical followed by 4X electronic amplification). The cells were then washed three times with PBS and lysed upon incubation for 1 hr at 37ºC with Triton X-100 (0.9% v/v in fresh phenol-free DMEM). The cell lysates were subsequently centrifuged for 2 hr at 4000 rpm (Eppendorf 5810R, Germany). The quantity of LDH was measured in the supernatant using the CytoTox 96® assay protocol (Promega Corporation, USA), following the manufacturer's instructions. Absorbance at 490 nm was measured in a FLUOstar Omega microplate reader (BMG Labtech, Germany). Cell viability was calculated as percentage of control untreated cells using the following equation: (A_{490} of treated cells - A_{490} of negative control) / (A_{490} of untreated cells - A_{490} of negative control) × 100 %.

In vitro phantom MR imaging

In vitro phantom MR imaging were performed at a 7T horizontal MR scanner (Agilent,

Palo Alto, CA). The gradient coil had an inner diameter of 12 cm, gradient strength of 1000 mT/m (100 G/cm) and rise-time of 120 μs. A quadrature transmit/receive coil (RAPID Biomedical GmbH, Germany) with an internal diameter of 39 mm was used. Phantom samples of SPION-GO were prepared in 1% agarose. A spin-echo MRI technique (where echo times (TE) were varied) was used to acquire T2-weigheted images *in vitro*. The spin-echo parameters in phantoms were: FOV = 30 × 30 mm, matrix size = 96 × 96, slice thickness = 1 mm; number of slice = 1; 1 average, TR = 2000 ms; TE = 10, 30, 50, 75, 100 and 125 ms; scan time ~20 min. MR images were analysed using the ImageJ software (NIH, USA).

Molecular Visualization

Molecular rendering was performed using Avogadro v1.1.1.[3] Molecular 3D visualization enhancement was performed using QuteMol.[4]

Statistical design of experiments (DoE) using two-level factorial design

Two-level full factorial design was used to screen the effect of three factors namely: milling frequency (A), milling time (B), and $RP_{Initial}$ (C) on the formulation process. The screening study for each factor was performed at low (-1) and high (+1) levels. The selection of the low and high values was based on the process capability of the instrument. Three replicated center points (0) were introduced to evaluate the potential curvature. The responses evaluated are M_{Total} and RP_{Final}. The design layout, data analysis (two-way ANOVA) and the generation of various 3D and contour graphs were achieved using Design-Expert® v.9 (Stat-Ease, Inc., USA). All experiments were carried out in strictly randomized order. Factors, models, and lack of fit test with a *p*-value below 0.05 were considered significant. The outputs of the experiments are referred to as "responses". As illustrated in **Figure S-1**, a cubic design space composed of factors A, B, and C, at high and low input levels were used. None of the design points is at the same condition as the other. The effects caused by each of the factors (E_A, E_B, and E_C) on the system were calculated from all the 8 design-points using **Equation S1**:

$$Effect = \frac{\sum Response_{Hi-livel}}{n_{Hi-level}} - \frac{\sum Response_{Lo-level}}{n_{Low-level}} \qquad \textbf{(S-1)}$$

where "*n*" is the number of experiments at each level. Effect from the two-factor interactions (E_{AB}, E_{BC}, and E_{AC}) were calculated using the same equation.[5] As shown in **Table S1**, factors were coded as +1 or -1 for high or low levels, respectively. Coding was

implemented so that the influence of the factors can be compared irrespective of the measurement unit. Three-replicated control runs i.e. center points (0) were introduced to estimate pure errors and to check for curvatures. A total of 11 experiments were performed (8 design points and 3 center points) in a random order to minimize bias.

The corded design layout is shown in **Table S2**. Two-factor interactions and three-factor interactions were calculated by multiplying the parent terms, *i.e.* $E_{AB} = E_A \times E_B$. Positive E_{AB} (+1) input were therefore, coming from STD 1 (−1 × −1 = 1), 4 (1 × 1 = 1), 5 (−1 × −1 = 1), and 8 (1 × 1 = 1). Two responses were measured, the M_{Total} (total hybrid weight) and the RP_{Final} (final GO/SPIO wt/wt % in the hybrid). M_{Total} and RP_{Final} were power-transformed with a λ at 0.5 (square root) and 0 (base 10 log), respectively; to yield relatively normal distributed data sets to get a minimal residual sum of squares in the transformed model. The power-transformed responses are shown in **Table S2**. Effect of main factors (A, B or C), the 2-factor (2 FI) or 3-factor (3FI) were calculated using **Equation S-1**.

An example for calculating the Effect of factor A (E_A) on the response M_{Total} is shown below:

$$E_A = \frac{77.53+95.83+20.46+26.82}{4} - \frac{107.10+125.71+44.50+50.15}{4} = -1.75$$

Analysis of response 1 (M_{Total})

The main effects, 2FI and 3FI of response 1 were calculated using **Equation S-1** and summarized in **Table S-2**. Half-normal plot was used to interpret the significance of the responses in 2-level factorial experiments. In brief, standardized effects were sorted in an ascending order then equally distributed across the accumulative half-normal plot. Normally distributed effects should line up as a straight line with ascending effect value, thus the observed effect fluctuation were due to random errors. Effects that did not follow the linear pattern indicated that these effects were unlikely caused by random errors. For M_{Total}, main effect A, B and C were all significant factors. None of the 2FI and 3FI was significant (**Figure S-2**). The residuals (the unselected factors) were tested by Shapiro-Wilk test. A p-value > 0.1 indicating the residuals were normally distributed. The main effects were therefore selected as model terms and tested by ANOVA. For a

balanced two-level factorial design, the sum of squares (SS) was calculated using **Equation S-2**, where *N* is the number of runs.

$$SS = \frac{N}{4}(Effect^2) \quad \textbf{(S-2)}$$

The non-normally distributed factors (A, B, and C) or terms will be used to construct the "model" for test response prediction. The sums of squares of the model (SS_{Model}) was therefore, expressed as the sum of squares of all out standing factors, as expressed in **Equation S-3**.

$$SS_{Model} = SS_A + SS_B + SS_C \quad \textbf{(S-3)}$$

Factors that have little effects were pooled as "residual" which was used as an estimated error, as expressed in **Equation S-4**.

$$SS_{Residual} = SS_{AB} + SS_{BC} + SS_{AC} \quad \textbf{(S-4)}$$

The mean squares (MS) were the SS divided by the degree of freedom (df). The F-value was the ratio of $MS_{Model}/MS_{Residual}$. The ANOVA result for response 1 (M_{Total}) is summarized in **Table S-3**. The model *F*-value of 111.49 indicates the model is significant (p < 0.0001), with only a 0.01% chance that this large *F*-value was caused by noise. Factor A, B, and C are model terms and all showed a significant effect on response 1 with a p-value of 0.0002, 0.0228 and < 0.0001, respectively. The lack of fit test *F*-value of 0.66 indicates that the lack of fit is not significant when compared to the pure error (p-value = 0.66).

Response 1 (M_{Total}) was then modeled with a predictive equation. Linear model was used to predict the power-transformed response. With 3 model terms (A, B, and C), the predictive equation is expressed as $\hat{Y} = \beta_0 + \beta_1 X_1 + \beta_2 X_2 + \beta_3 X_3$, where $\hat{Y}$ is the predicted response. The model coefficient β_0 is the intercept, representing the average of all observed responses (power-transformed, as summarised in **Table S-2**). The model coefficients *e.g.* β_1, β_2 and β_3, represents the slope of the response. As shown in **Equation S-1**, factor effects indicate the change of responses when the factor goes from

low-level (-1) to high-level (+1). The factor coefficient *i.e.* the slope can then be calculated using **Equation S-5**.

$$Factor\ cofficient = \frac{Factor\ effect}{Change\ in\ factor\ level} = \frac{Factor\ effect}{1-(-1)} = \frac{Factor\ effect}{2} \quad \textbf{(S-5)}$$

The estimated regression coefficients for response 1 (M_{Total}) are summarized in **Table S-4**. The final fitted model for the M_{Total} with the coded factors of milling frequency (A), milling time (B), and $RP_{Initial}$ (C) is shown in **Equation 1**.

Analysis of response 2, (RP_{Final})

The half normal probability plot of the absolute standardized effects for M_{Total} is shown in **Figure S-4**. Only factor C was identified as the factor with non-normally distributed (significant) effect. Factor A and B, however, were still included as model terms to help improve the prediction and to evaluate their inputs. The residuals (the unselected factors) were tested by Shapiro-Wilk test. A p-value > 0.1 indicated that the residuals were normally distributed. The main effects, as the model terms, were then tested by ANOVA. For a balanced two-level factorial design, the sum of squares (SS) was calculated using **Equation S-2**, where N is the number of runs. The sum of squares of the model (SS_{Model}) was calculated using **Equation S-3**. Factors that have little effects were pooled as "residual" and was used as an estimated error and calculated using **Equation S-4**. The mean squares (MS) were the SS divided by the degree of freedom (df). The F-value was the ratio of $MS_{Model}/MS_{Residual}$. The ANOVA result for response 2 (RP_{Final}) is summarized in **Table S-5**. The model F-value of 39.18 indicates that the model is significant (p < 0.0001), with only a 0.01% chance that this large F-value was caused by noise. Factor C is the significant model term with a p-value < 0.0001. Factors A and B were not significant with a p-value of 0.0587 and 0.1267, respectively. Factor C ($RP_{Initial}$) is the dominating factor towards RP_{Final}, and the only factor that had a significant influence (p-value < 0.05). The lack of fit test F-value of 0.71 indicates that the lack of fit is not significant when compared to the pure error (p-value = 0.6745).

Response 2 (RP_{Final}) was then modeled with predictive equation, as described for Response 1. The estimated coefficients of the model terms are summarized in **Table S-6**.

The final fitted model for the RP_{Final} with the coded factors of milling frequency (A), milling time (B), and $RP_{Initial}$ (C) is showed in **Equation 3**.

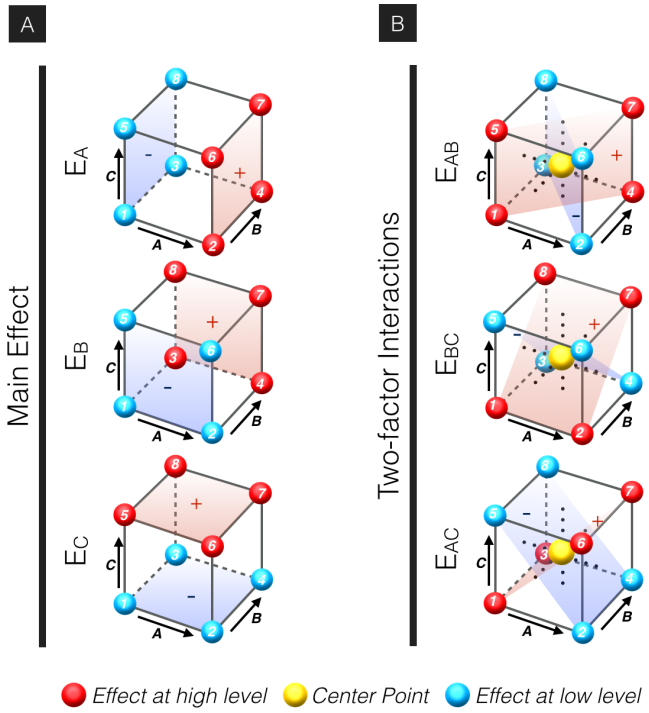

Figure S-1. Schematic illustration of calculating the main effects and two-factor interactions (2FI), in a two-level full factorial design, also represented in Equation S1.

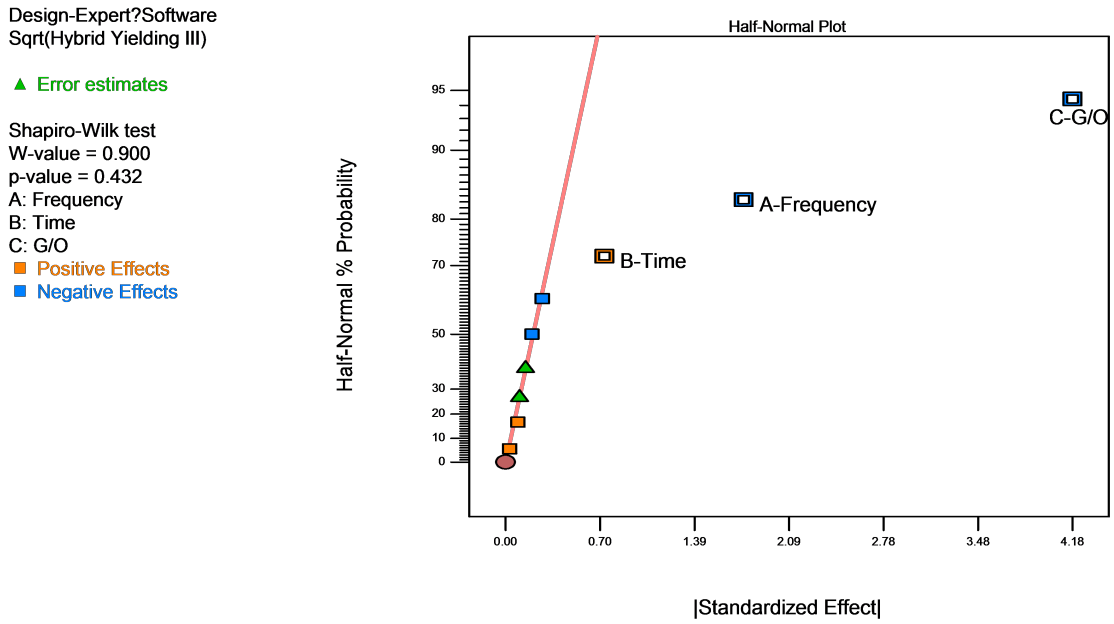

Figure S-2. Use of half-normal plot in interpreting Response 1 in a 2-level factorial experiments. Standardized effects were equally distributed across the accumulative probability, normally distributed effects should line up as a straight line with ascending effect value. Effects that did not follow the linear pattern indicated that these effects were unlikely caused by random errors.

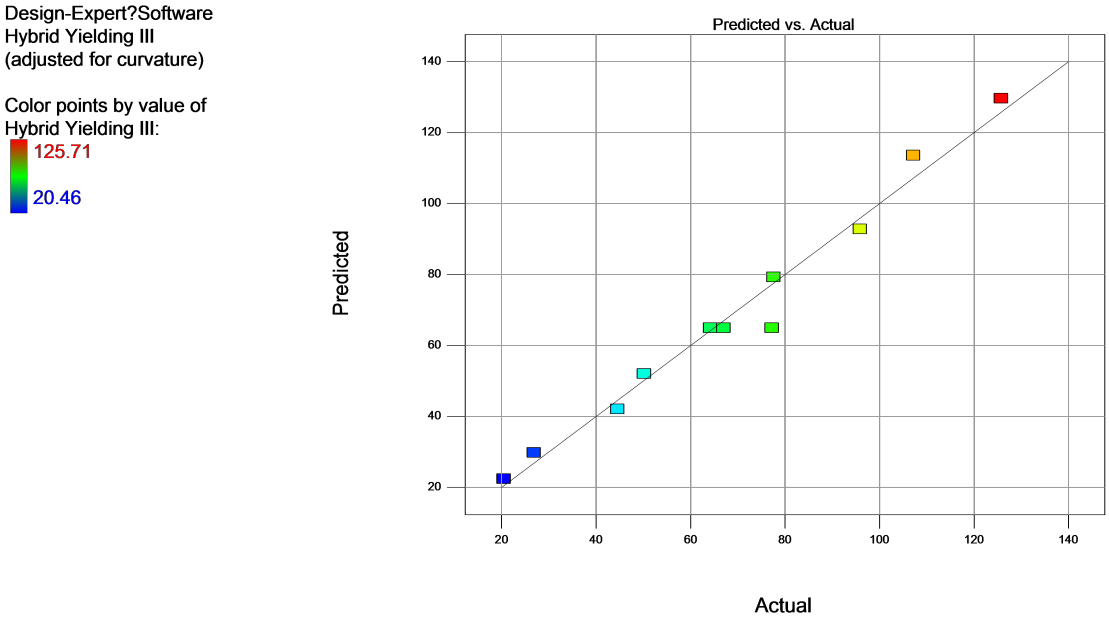

Figure S-3. Comparison of the predicted and actual (experimental) values for Response 1.

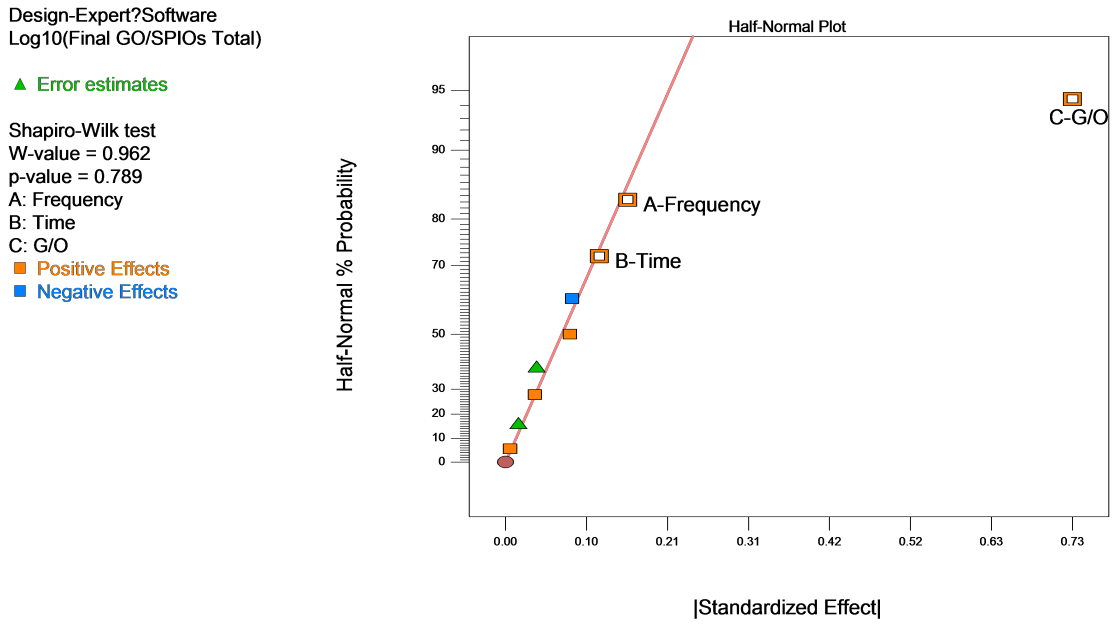

Figure S-4. Use of half-normal plot in interpreting Response 2 in a 2-level factorial experiments. Standardized effects were equally distributed across the accumulative probability, normally distributed effects should line up as a straight line with ascending effect value. Effects that did not follow the linear pattern indicated that these effects were unlikely caused by random errors. Factor C in this case was the only significant factor, however, Factors A and B were still included in the model to improve the prediction and evaluate their input.

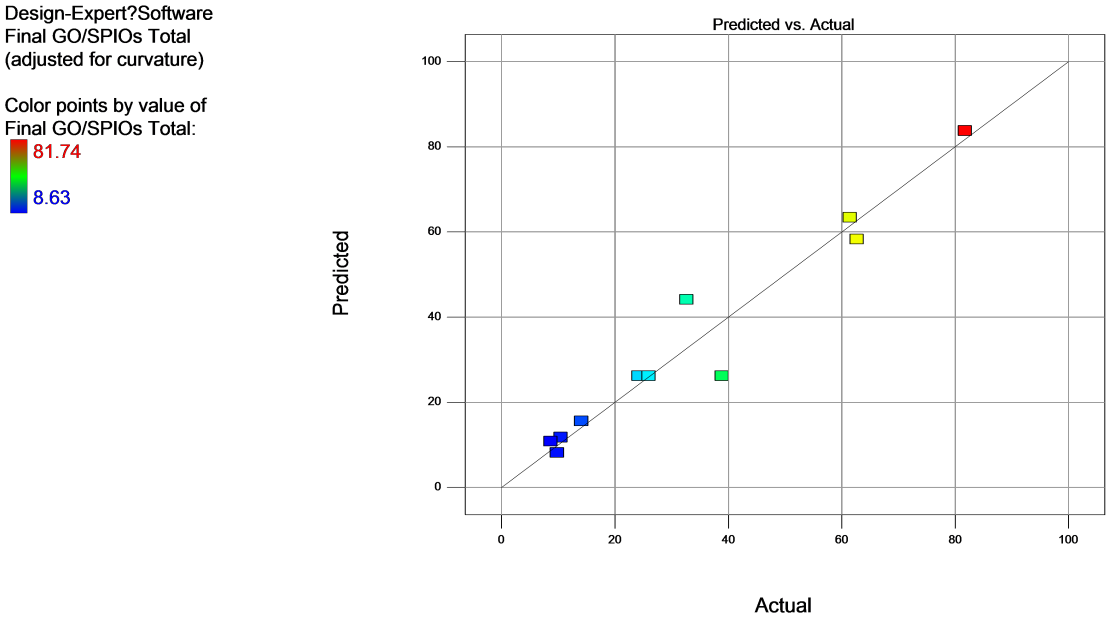

Figure S-5. Comparison of the predicted and actual (experimental) values for Response 2.

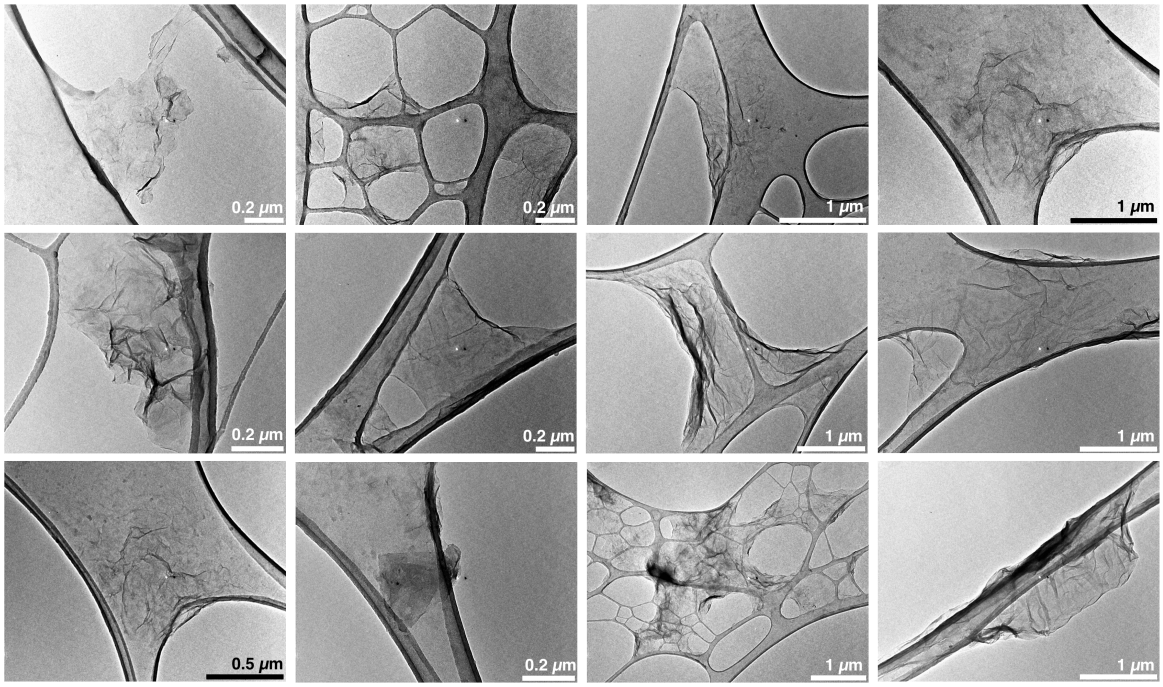

Figure S-6. TEM images of GO. The TEM images of single layer GO sheet on a lacey carbon support are shown.

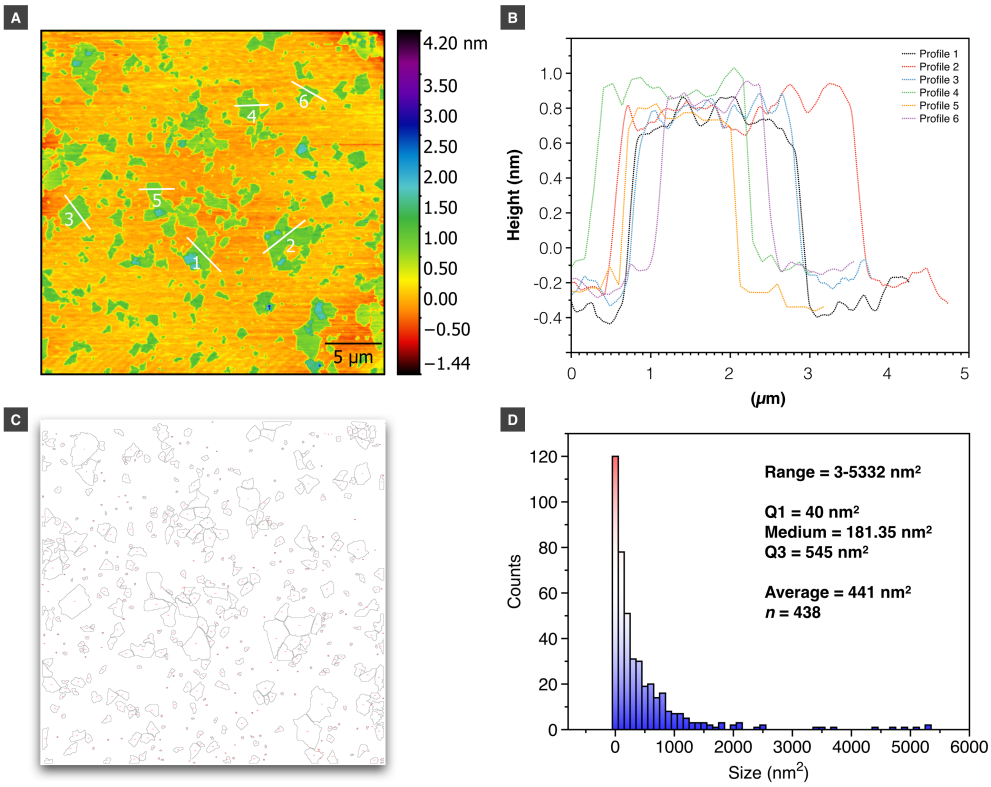

Figure S-7. GO morphological observation using AFM. (A) AFM height images of as-synthesised GO with uniform height of ~1 nm. **(B)** Cross-section height analysis of GO sheets confirming the height/thickness of around 1 nm thus the presence of single layer GO sheets. **(C)** Image analysis for surface area measurement using ImageJ. **(D)** Surface area distribution of as-synthesised GO sheets obtained from images in C.

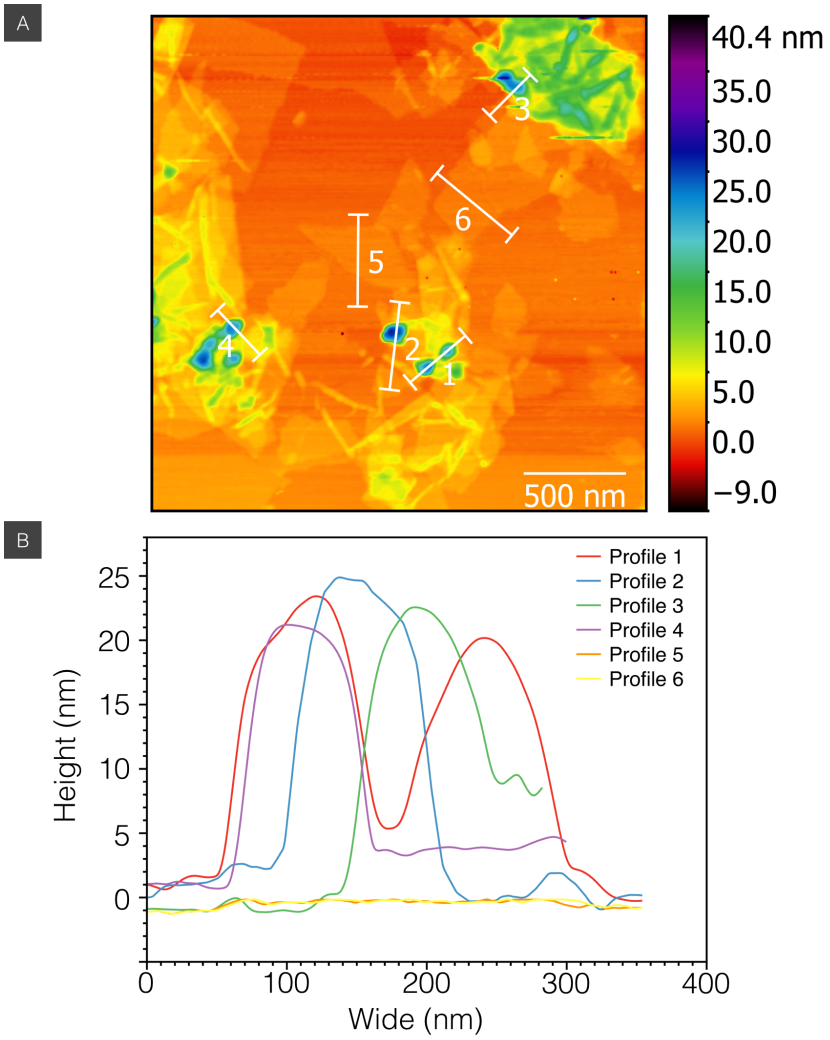

Figure S-*8*. GO-SPIOs morphological observation using AFM. (A) AFM height images of GO-SPIOs. **(B)** Cross-section height analysis of GO-SPIOs showing heights between 10-20 nm. The height matches the theoretical size of SPIOs.

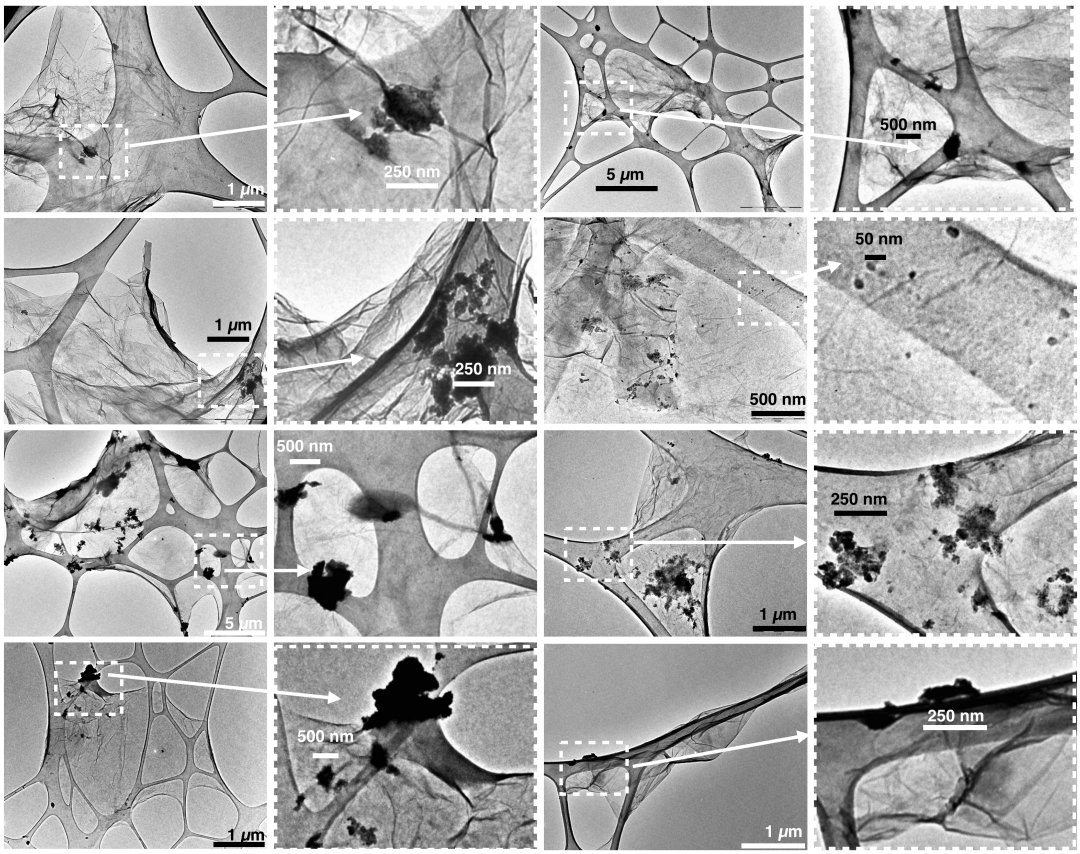

Figure S-9. TEM images of GO/SPIOs hybrids with larger aggregated particles. Despite a good number of 10-20 nm SPIOs were found in the hybrid (as shown in **Figure 2**), some larger aggregated particles were also found to be associated with GO. As SPIOs aggregate without solvents, this is expected and was acknowledged as one of the limitations of the ball-milling approach. Cryo-mill or ball-mills with higher grinding power may help to decrease the aggregation of SPIOs when using a solvent-free approach.

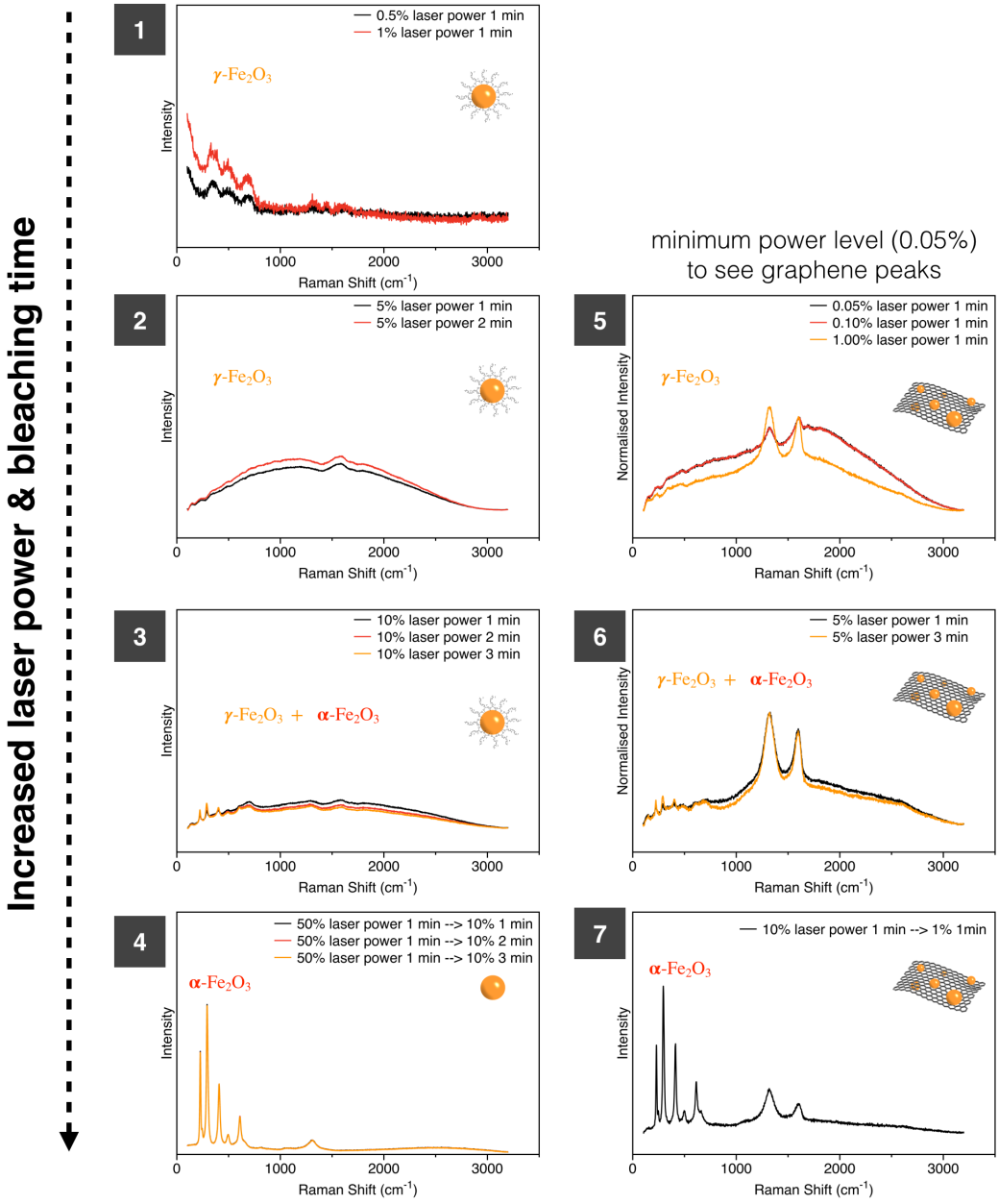

Figure S-10. Raman spectra of SPIOs and GO/SPIO hybrids. (1-4) SPIOs can undergo phase transformation when exposed to higher laser powers during Raman spectrum acquisition. For example, γ-Fe_2O_3 (maghemite) could be transformed to α- Fe_2O_3 (hematite) when the laser power increased from 0.5 % to 50 %. **(5-7)** The phase transformation can be observed in GO/SPIO hybrids when a much lower laser power was used. The presence of SPIOs in the hybrid can be confirmed by transforming the γ-Fe_2O_3 into α-Fe_2O_3, which gives a much stronger Raman signal.

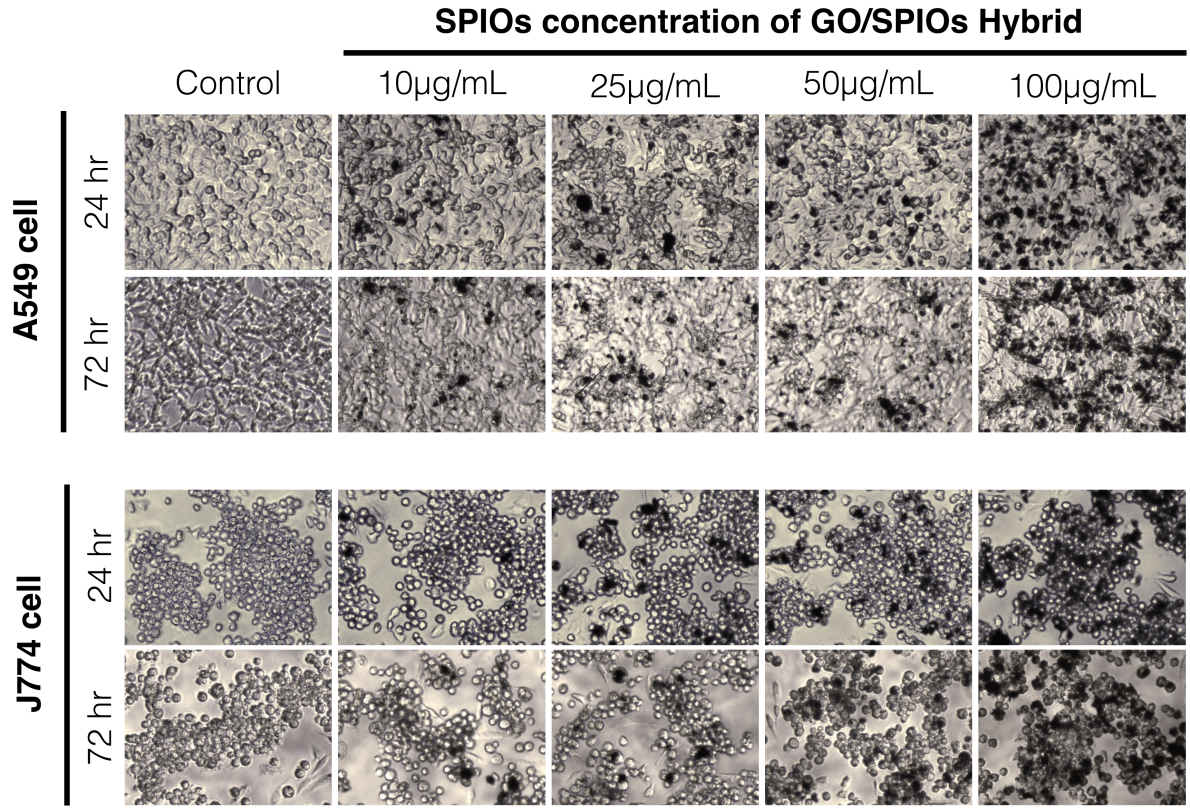

Figure S-11. Optical microscopy images of A549 and J774 cells incubated with GO/SPIO hybrids. Cells were incubated with GO/SPIOs hybrids at a SPIOs concentration of 10, 50, and 100 μg/mL for 72 hr at 37 °C. Normal morphology was observed at all concentrations tested, while cells treated with DMSO appeared unhealthy and detached from the plate. As shown by the dark signals localised to cells, the extent of GO/SPIO hybrids uptake was concentration- and time-dependent.

Table S-1. Test factors for making GO/SPIO hybrids with actual and coded levels.

Factor	Name	Unit	Low Level (-1)	Centre Point (0)	High Level (+)
A	Frequency	Hz	10	15	20
B	Time	Hr	1	1.5	2
C	$RP_{Initial}$	Wt/Wt %	25	50	75

Table S-2. Full 2^3 (two-level, three factors) factorial design.

Std. No.	Factor			2FI			3FI	Response[a]	
	A	B	C	E(AB)	E(BC)	E(AC)	E(ABC)	$(M_{Total})^{0.5}$	$Log(RP_{Final})$
1	-1	-1	-1	1	1	1	-1	10.35	0.99
2	1	-1	-1	-1	1	-1	1	8.81	1.02
3	-1	1	-1	-1	-1	1	1	11.21	0.94
4	1	1	-1	1	-1	-1	-1	9.79	1.15
5	-1	-1	1	1	-1	-1	1	6.67	1.51
6	1	-1	1	-1	-1	1	-1	4.52	1.79
7	-1	1	1	-1	1	-1	-1	7.08	1.80
8	1	1	1	1	1	1	1	5.18	1.91
9[b]	0	0	0	0	0	0	0	8.18	1.38
10[b]	0	0	0	0	0	0	0	8.01	1.59
11[b]	0	0	0	0	0	0	0	8.79	1.41
Effect on $(M_{Total})^{0.5}$ [c]	-1.75	0.73	-4.18	0.09	-0.20	-0.27	0.03	8.05[d]	–
Effect on $Log(RP_{Final})$ [c]	0.16	0.12	0.73	0.01	0.08	0.04	-0.09	–	1.41[d]

[a] Responses are power transformed. [b] Repeated center points. [c] Calculated by Equation S1.

[d] Calculated from the mean transformed response value of Std. No.1-11.

Table S-3. Analysis of variance (ANOVA) for response 1 (M_{Total}).

Source	Sum of Squares	df	Mean Square	*F*-value	*p*-value	
Model	42.08	3	14.03	111.49	<0.0001	*significant*
A	6.15	1	6.15	48.92	0.0002	
B	1.06	1	1.06	8.43	0.0228	
C	34.86	1	34.86	277.10	<0.0001	
Residual	0.88	7	0.13			
Lack of Fit	0.55	5	0.11	0.66	0.6944	*not significant*
Pure Error	0.33	2	0.17			
Cor Total	42.96	10				

Table S-4. Estimated regression coefficients for response 1 (M_{Total}).

Factor	Coefficient (coded)	df	Standard Error	*95% CI Low*	*95% CI High*	VIF
Intercept	8.05	1	0.11	7.80	8.31	
A	-0.88	1	0.13	-1.17	-0.58	1
B	0.36	1	0.13	0.07	0.66	1
C	-2.09	1	0.13	-2.38	-1.79	1

Table S-5. Analysis of variance (ANOVA) for response 2 (RP_{Final}).

Source	Sum of Squares	df	Mean Square	*F*-value	*p*-value	
Model	1.14	3	0.38	39.18	<0.0001	*significant*
A	0.05	1	0.05	5.09	0.0587	
B	0.03	1	0.03	3.00	0.1267	
C	1.07	1	1.07	109.44	<0.0001	
Residual	0.07	7	0.01			
Lack of Fit	0.04	5	0.01	0.71	0.6745	*not significant*
Pure Error	0.03	2	0.01			
Cor Total	1.21	10				

Table S-6. Estimated regression coefficients for response 2 (RP_{Final}).

Factor	Coefficient (coded)	df	Standard Error	*95% CI Low*	*95% CI High*	VIF
Intercept	1.41	1	0.030	1.34	1.48	
A	0.08	1	0.035	-0.004	0.16	1
B	0.06	1	0.035	-0.022	0.14	1
C	0.37	1	0.035	0.28	0.45	1

References:

(1) Kovtyukhova, N. I.; Ollivier, P. J.; Martin, B. R.; Mallouk, T. E.; Chizhik, S. A.; Buzaneva, E. V.; Gorchinskiy, A. D. Layer-by-Layer Assembly of Ultrathin Composite Films From Micron-Sized Graphite Oxide Sheets and Polycations. *Chem. Mater.* **1999**, *11*, 771–778.

(2) Nečas, D.; Klapetek, P. Gwyddion: an Open-Source Software for SPM Data Analysis. *centr.eur.j.phys.* **2011**, *10*, 181–188.

(3) Hanwell, M. D.; Curtis, D. E.; Lonie, D. C.; Vandermeersch, T.; Zurek, E.; Hutchison, G. R. Avogadro: an Advanced Semantic Chemical Editor, Visualization, and Analysis Platform. *J Cheminf* **2012**, *4*, 17–17.

(4) Tarini, M.; Cignoni, P.; Montani, C. Ambient Occlusion and Edge Cueing for Enhancing Real Time Molecular Visualization. *Visualization and Computer Graphics, IEEE Transactions on* **2006**, *12*, 1237–1244.

(5) Novoselov, K. S. Nobel Lecture: Graphene: Materials in the Flatland. *Rev. Mod. Phys.* **2011**, *83*, 837–849.